New Horizons Mapping of Europa and Ganymede
W. M. Grundy, *et al.*
Science **318**, 234 (2007);
DOI: 10.1126/science.1147623

process can act to truncate the size distribution. In erosive processes, dr/dt is a constant, independent of r. Hence, in the same time that Metis shrinks from $r = 27$ to 22 km, all 5-km bodies in the system would vanish (Fig. 4). This explanation requires that reaccretion be negligible, which is reasonable so deep inside Jupiter's Roche limit.

Earlier images from Voyager and Galileo showed longitudinal asymmetries on a scale much larger than the tiny clumps found by New Horizons (*6*, *7*, *12*). The absence such large features in the recent data is puzzling; perhaps seasonal or other time-scale variations play a role. Cassini images found one hint of smaller-scale clumping in the jovian ring (*13*). An arc ~ 8° in length appeared near the outer edge of the rings in three low-phase images, leading Adrastea at the time by ~4°. The epoch was ~0:00 UTC on 13 December 2000. We can extrapolate our clump motions backward for the intervening 2265 days to determine that features α and β fell 232° ± 39° and 226° ± 72° ahead of Adrastea (*14*). Unless unknown orbital perturbations are at work, these families can both be ruled out as the feature imaged by Cassini; apparently, that feature no longer exists. Cassini's images had lower resolution and SNR, however, so we cannot rule out α and β as long-lived features that were too small for Cassini to detect.

The presence of these clumps challenges our theoretical understanding. By Kepler shear, a 1-km-wide clump at α's orbit will spread 5.1° in 1 year; this distance is far larger than the few tenths of a degree of individual clumps. This leaves two alternatives: either the clump families are young or they are actively confined. Transient features could be explained by impacts from meteoroids or by collisions among the ring members. If the clumps are spreading, then this would provide an unambiguous indicator of their youth. Of the two clumps with best-determined orbits, α1 and α3 (Table 1), the leading clump appears to be moving slightly faster, suggesting that they might have emerged from a single point ~ 90 days before the flyby. However, the mean motions are too uncertain to rule out a much longer lifetime. Of course, a recent impact should generate substantial dust, such as is widely seen in Saturn's F ring (*15*–*18*), but Jupiter's clumps are not dusty. Also, an impact would be expected to produce one broad arc rather than the multiple, seemingly uniformly spaced clumps seen in the α family.

Alternatively, the 1.8° periodicity of clumps in group α is suggestive of a resonant confinement mechanism, perhaps comparable to Galatea's effects on the Adams ring of Neptune (*19*, *20*). Metis' resonances probably dominate; although it orbits three times as far away from the clumps as Adrastea, Metis is ~20 times more massive. Notably, Metis' 115:116 corotation inclination resonance falls at 128736.9 km, just 0.8 km from the orbit of the α family. Also, its adjacent 114:115 resonance falls at 128743.6 km, which is 0.6 km from the orbit of the β family. With 6.7 km between resonances, the probability that both families would fall so close to resonant locations by random chance is 4% (although the orbits have relatively larger uncertainties). However, these resonances are expected to confine material at intervals of ~ 180°/115 = 1.56°, which does not match the observed clump spacings. Nevertheless, the clumps in Neptune's Adams ring also do not show the predicted periodicities, suggesting that our understanding of resonant confinement remains incomplete.

The jovian ring's large-scale asymmetries have now vanished, but different, much smaller structures have been revealed. This follows upon observations that the radial structure of Saturn's equally faint D ring has changed radically in the past 25 years; some features have faded and spread, whereas other regions show entirely new structure (*21*). Similarly, the uranian ζ ring has recently been found to have shifted radially since the 1986 Voyager flyby (*22*). We conclude that the general class of dusty rings may be much more dynamic and time-variable than was previously supposed, with variations on 10- to 20-year time scales not the exception but the norm.

References and Notes

1. J. A. Burns, M. R. Showalter, J. N. Cuzzi, J. B. Pollack, *Icarus* **44**, 339 (1980).
2. J. A. Burns, M. R. Showalter, G. Morfill, in *Planetary Rings*, R. Greenberg, A. Brahic, Eds. (Univ. Arizona Press, Tucson, 1984), pp. 200–272.
3. J. A. Burns *et al.*, in *Jupiter: The Planet, Satellites and Magnetosphere*, F. Bagenal, T. E. Dowling, W. B. McKinnon, Eds. (Cambridge Univ. Press, Cambridge, 2004), pp. 241–262.
4. M. R. Showalter, J. A. Burns, I. de Pater, D. P. Hamilton, M. Horanyi, *Bull. Am. Astron. Soc.* **35**, #11.08 (2003).
5. I. de Pater *et al.*, *Icarus* **138**, 214 (1999).
6. M. R. Showalter, J. A. Burns, J. N. Cuzzi, J. B. Pollack, *Icarus* **69**, 458 (1987).
7. M. Ockert-Bell *et al.*, *Icarus* **138**, 188 (1999).
8. C. C. Porco, Cassini Imaging Team, *Int. Astron. Union Circ.* #8242 (2005).
9. J. N. Spitale, R. A. Jacobson, C. C. Porco, J. W. M. Owen, *Astron. J.* **132**, 692 (2006).
10. C. C. Porco, Cassini Imaging Team, *Int. Astron. Union Circ.* #8857 (2007).
11. R. M. Canup, L. W. Esposito, *Icarus* **113**, 331 (1995).
12. S. M. Brooks, L. W. Esposito, M. R. Showalter, H. B. Throop, *Icarus* **170**, 35 (2004).
13. H. B. Throop *et al.*, *Icarus* **172**, 59 (2004).
14. C. C. Porco *et al.*, *Science* **299**, 1541 (2003).
15. M. R. Showalter, *Science* **282**, 1099 (1998).
16. M. R. Showalter, *Icarus* **171**, 356 (2004).
17. J. M. Barbara, L. W. Esposito, *Icarus* **160**, 161 (2002).
18. S. Charnoz *et al.*, *Science* **310**, 1300 (2005).
19. C. C. Porco, *Bull. Am. Astron. Soc.* **22**, #1043 (1990).
20. F. Namouni, C. C. Porco, *Nature* **417**, 45 (2002).
21. M. M. Hedman *et al.*, *Icarus* **188**, 89 (2007).
22. I. de Pater, H. B. Hammel, M. R. Showalter, M. A. van Dam, *Science* **317**, 1888 (2007).

23. We thank the entire New Horizons mission team and our colleagues on the New Horizons science team. New Horizons is funded by NASA, whose financial support we acknowledge.

11 July 2007; accepted 19 September 2007
10.1126/science.1147647

REPORT

New Horizons Mapping of Europa and Ganymede

W. M. Grundy,[1*] B. J. Buratti,[2] A. F. Cheng,[3] J. P. Emery,[4] A. Lunsford,[5] W. B. McKinnon,[6] J. M. Moore,[7] S. F. Newman,[2] C. B. Olkin,[8] D. C. Reuter,[5] P. M. Schenk,[9] J. R. Spencer,[8] S. A. Stern,[10] H. B. Throop,[8] H. A. Weaver,[3] and the New Horizons team

The New Horizons spacecraft observed Jupiter's icy satellites Europa and Ganymede during its flyby in February and March 2007 at visible and infrared wavelengths. Infrared spectral images map H_2O ice absorption and hydrated contaminants, bolstering the case for an exogenous source of Europa's "non-ice" surface material and filling large gaps in compositional maps of Ganymede's Jupiter-facing hemisphere. Visual wavelength images of Europa extend knowledge of its global pattern of arcuate troughs and show that its surface scatters light more isotropically than other icy satellites.

NASA's Voyager and Galileo space probes revealed the icy Galilean satellites to be distinct, complex worlds with surfaces geologically and chemically sculpted by diverse endogenic and exogenic processes (*1*, *2*). Many outstanding questions remain regarding the composition and biological potential of Europa's interior ocean and the nature of its icy crust, the existence of possible oceans within Ganymede and Callisto, and the composition of enigmatic "non-ice" material on Europa and Ganymede that distorts their H_2O ice absorption bands (*3*–*5*).

During its 2007 flyby of Jupiter, New Horizons (*6*) observed Europa, Ganymede, and Callisto (table S1) with its infrared (1.25 to 2.5 μm) Linear Etalon Imaging Spectral Array (LEISA) (*7*) and its panchromatic (0.35 to 0.85 μm) LOng-Range Reconnaissance Imager (LORRI) charge-coupled device camera (*8*). LEISA observations used spacecraft motion to slew the field of view across

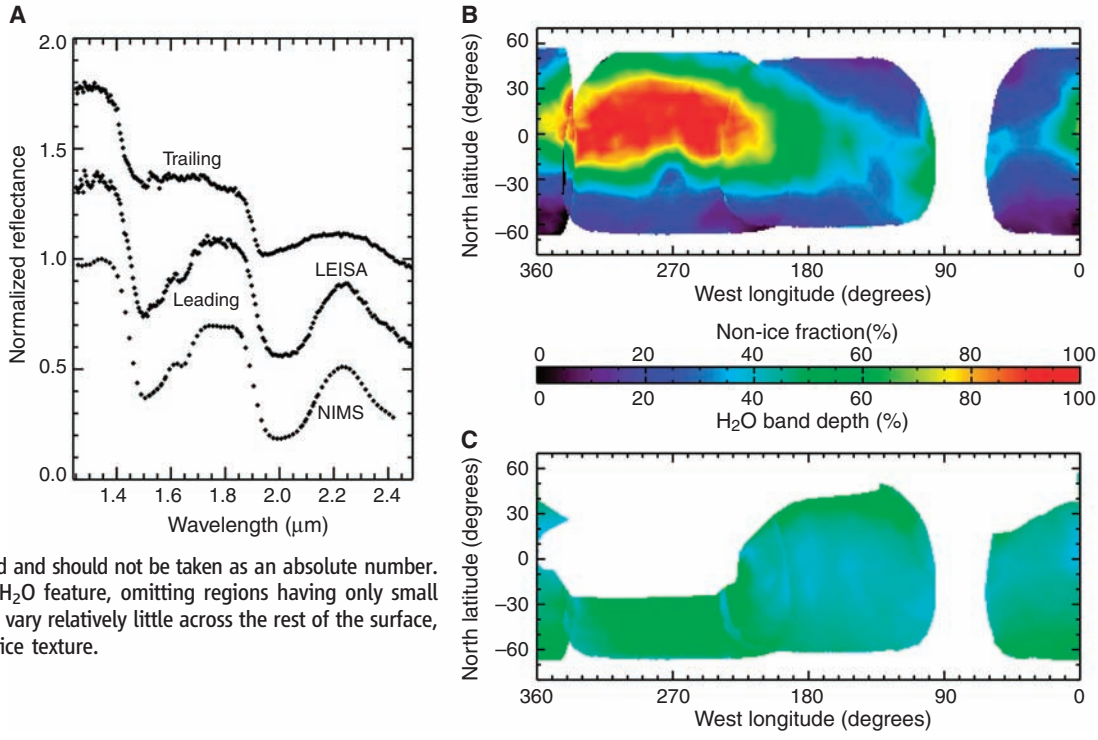

Fig. 1. LEISA compositional mapping of Europa. (**A**) Example spectra, top to bottom: LEISA trailing hemisphere spectrum showing distorted H_2O bands, then LEISA and NIMS (*5*) leading hemisphere spectra showing cleaner H_2O ice. These examples illustrate LEISA data quality and the spectral variability of Europa's surface. Upper spectra are offset by +0.4 and +0.8. Uncertainties are indicated by the scatter. (**B**) Spatial distribution of the "non-ice" material that distorts Europa's H_2O bands. Highest concentrations (in red, as indicated by the shared color bar) occur near the trailing apex (270°W, 0°N). The fraction depends on the specific end-members selected and should not be taken as an absolute number. (**C**) Depth of the 2-μm residual H_2O feature, omitting regions having only small fractions of pure ice. Band depths vary relatively little across the rest of the surface, indicative of homogeneous H_2O ice texture.

the target to build up spectral image cubes. LORRI observations consist of single images or pairs of images with bracketing exposure times made in a point-and-stare framing mode. During the several-day close approach phase, Ganymede and Callisto remained on the far side of Jupiter from New Horizons, limiting the spatial resolution achievable but allowing study of their Jupiter-facing hemispheres, including regions of Ganymede poorly mapped by Galileo's Near-Infrared Mapping Spectrometer (NIMS). Europa's more rapid orbital motion enabled compositional mapping of most of its surface.

Europa's distorted H_2O vibrational absorption band shapes are attributed to water of hydration, but the composition and origin of the hydrated material are unresolved. Association with lineae, chaos regions, and possible erup-

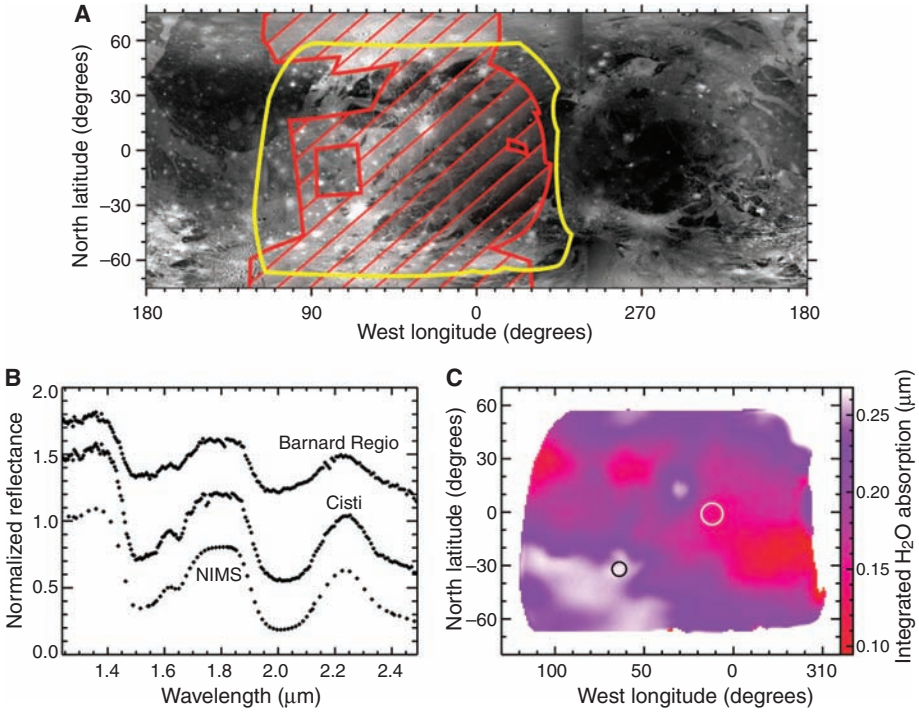

Fig. 2. LEISA compositional mapping of Ganymede. (**A**) Regions of Ganymede not mapped by NIMS (red hatches) and mapped by LEISA (yellow outline). (**B**) Example spectra, top to bottom: LEISA spectra of Barnard Regio (10°W, 2°S) and of the bright, rayed crater Cisti (64°W, 32°S) compared with NIMS spectrum of an ice-rich region (*27*). The spectra are normalized at 1.8 μm and offset by +0.6, +0.2, and −0.2, respectively. (**C**) Map of integrated absorption by the 1.5- and 2-μm H_2O ice bands. Regions around Cisti (black circle) and Barnard Regio (white circle) contributed to the LEISA average spectra in (B).

[1]Lowell Observatory, 1400 West Mars Hill Road, Flagstaff, AZ 86001, USA. [2]Jet Propulsion Laboratory, 4800 Oak Grove Drive, Pasadena, CA 91109, USA. [3]Johns Hopkins University Applied Physics Laboratory, 11100 Johns Hopkins Road, Laurel, MD 20723, USA. [4]SETI Institute/NASA Ames Research Center, 515 North Whisman Road, Mountain View, CA 94043, USA. [5]NASA Goddard Space Flight Center, Code 693, Greenbelt, MD 20771, USA. [6]Department of Earth and Planetary Science, Washington University, Campus Box 1169, 1 Brookings Drive, St. Louis, MO 63130, USA. [7]NASA Ames Research Center, MS 245-3, Moffett Field, CA 94035, USA. [8]Department of Space Studies, Southwest Research Institute, 1050 Walnut Street, Suite 300, Boulder, CO 80302, USA. [9]Lunar and Planetary Institute, 3600 Bay Area Boulevard, Houston, TX 77058, USA. [10]NASA Science Mission Directorate, NASA Headquarters, Washington, DC 20546, USA.

*To whom correspondence should be addressed. E-mail: w.grundy@lowell.edu

tions raise the possibility that the hydrated material came from Europa's interior ocean (*3*–*5*). Compositional interpretations favoring hydrated magnesium and/or sodium sulfate or sulfide salts might then constrain ocean chemistry and potential to host life (*9*, *10*). However, exogenic sulfur from Io (or from endogenic salts) was shown to be rapidly modified on Europa's surface by charged particles from the jovian magnetosphere, leading to a radiolytic sulfur cycle on thousand-year time scales between elemental sulfur, sulfur dioxide, and sulfuric acid, which is also a good spectral match for the "non-ice" material (*11*–*14*).

New Horizons made three LEISA observations of Europa with subspacecraft pixel scales from 250 to 180 km, corresponding to 120 to 230 pixels on the disk of Europa. The observations included the trailing hemisphere where the "non-ice" material was known to be more abundant (*13*). The spectral resolution of LEISA ($\lambda/\Delta\lambda \approx 240$) is potentially high enough to distinguish contending hydrated salt and acid species (*14*), but calibration procedures for LEISA data are still being refined, so we will concentrate on the two strong H_2O ice absorption complexes at ~1.5 and 2.0 μm that dominate the spectra (Fig. 1A).

We mapped the distribution of distorted H_2O bands by using a simple mixing model with two components derived by averaging several distorted spectra for one end-member and several clean ice-like spectra for the other. The resulting map (Fig. 1B) confirms previous results (*4*, *13*) and extends coverage substantially, showing that the band-distorting material is distributed symmetrically about the apex of the trailing hemisphere (270°W, 0°N). This pattern is consistent with implantation of sulfur from Io and of bombardment by magnetospheric charged particles (*15*). Our "non-ice" map also matches the distribution of an ultraviolet absorber, possibly sulfur, mapped from Voyager data (*16*). The main deviation from this symmetry in both maps is an area of cleaner ice south of the trailing apex associated with ejecta from the young, bright, rayed crater Pwyll (271°W, 25°S). That Pwyll ejecta contains less "non-ice" is consistent with an exogenic source for that material. However, instances of local geographical control of the "non-ice" material (*4*, *13*) imply at least some endogenic influence on its formation or preservation.

Removing appropriate fractions of distorted-band material from each pixel leaves residual H_2O spectra. The residual absorption bands measure the mean optical path length traversed within H_2O ice. A band depth map (Fig. 1C) shows little regional variation, implying relatively consistent ice textures across the surface of Europa. Processes governing ice texture evidently lack the strong hemispheric asymmetry of the processes responsible for the distribution of "non-ice" material.

New Horizons targeted Ganymede's subjovian hemisphere (Fig. 2A), including bright, rayed craters Cisti (64°W, 32°S), Tros (27°W, 11°N), and Shu (3°E, 43°N), as well as darker Nicholson Regio (50°W to 40°E, 10°S to 50°S), Barnard Regio (20°W to 10°E, 10°S to 10°N), and Perrine Regio (70°W to 0°W, 10°N to 50°N). The 1.65-μm H_2O ice band, characteristic of low-temperature crystalline ice (*17*), is well resolved by LEISA (Fig. 2B). Some regions of Ganymede's trailing hemisphere were reported to exhibit H_2O band asymmetries like Europa's "non-ice" (*5*). Asymmetric bands are also apparent in LEISA spectra, especially of darker areas. Subtle dips suggestive of hydrates appear around 1.4, 1.7, and 1.8 μm (*14*), but their interpretation awaits improved calibration. Comparison of an H_2O absorption map (Fig. 2C) with the context map (Fig. 2A) shows greater H_2O ice absorption associated with brighter regions and with recent impacts and their ejecta. The bright, heavily cratered, leading-hemisphere region south of 20°S and west of 40°W shows particularly strong H_2O absorption. This correlation is consistent with accumulation at the surface of a globally distributed dark material except where relatively recent impacts have excavated cleaner ice from below the surface.

LORRI panchromatic images of the satellites with spatial resolutions of 15 to 30 km/pixel reveal no changes since Galileo images ~5 years earlier. Processes that modify surfaces at large spatial scales, such as impacts of kilometer-sized bodies, are highly unlikely during that interval [$<10^{-5}$ probability (*18*)].

LORRI images surveyed Europa's large-scale arcuate troughs, which are notable for their scale and their symmetry. They form two sets of concentric small circles with centers at antipodal points 300°W, 10°N and 120°W, 10°S. From Galileo imaging and image-derived digital terrain models, they are up to ~50 km wide and from several hundred meters to more than a kilometer deep (*19*). They do not distort or displace other, intersecting surface albedo and tectonic features and are not obviously related to other tectonic patterns identified on Europa (*20*).

The New Horizons trajectory provided low Sun elevation, near-normal views of Europa's trailing hemisphere terminator, enabling us to target gaps in comparable Galileo coverage. LORRI images reveal a predicted northward extension (*19*) of the trough segment near 340°W longitude (Fig. 3), confirming

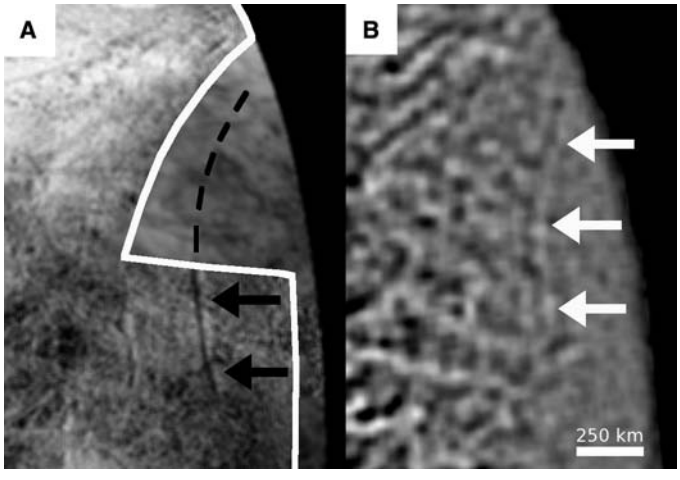

Fig. 3. Large-scale arcuate troughs on Europa. (**A**) Arrows mark the 340°W trough segment detected in Galileo images. Galileo only observed the region to the left of the white curve at suitable illumination geometry to reveal these features. Dashes indicate the predicted continuation of the trough (*19*). (**B**) A highly stretched New Horizons LORRI image of the same region (roughly 10°W to 30°E, 10°S to 45°N, with north up) reveals the continuation of the trough (white arrows).

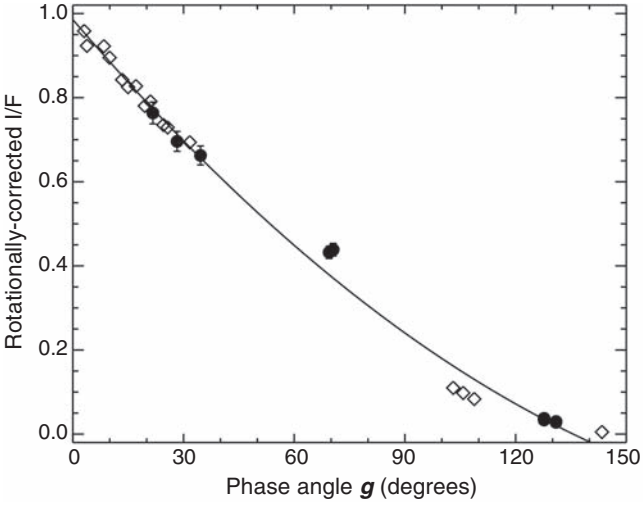

Fig. 4. LORRI disk-integrated photometry of Europa. New Horizons observations (filled circles, with 1-σ error bars) are consistent with Voyager measurements (open diamonds). A second-order polynomial $y(g) = c + bg + ag^2$ (smooth curve) approximates the data with $b = -0.01$ and $a = 2.2 \times 10^{-5}$.

that the troughs are a truly global phenomenon. No trough was seen near longitude 270°W, but that region is geologically complex, with numerous criss-crossing dark lineaments. The north-south offset of the antipodal centers of symmetry, maintained in the New Horizons images, hints at true polar wander of Europa's ice shell (*21*–*23*).

From Earth, the solar phase angle g for the Jupiter system is ≤12°, limiting Earth-based measurement of directional scattering by jovian satellites. Only spacecraft can access higher phase angles. LORRI observed the Galilean satellites at a range of phase angles (table S1), filling gaps in Europa's solar phase curve between 32° and 103° and between 109° and 143°. The photometric data, corrected for longitudinal variations and normalized to Voyager data (*24*), are shown in Fig. 4. Europa's brightness at $g = 70°$ is more than 40% of its fully illuminated brightness, underscoring the unique texture of its surface produced by active resurfacing. The comparable number for Earth's Moon is only 20%.

Our observations improve measurement of Europa's phase integral q, which describes the directional scattering properties of light reflected from its surface. The new q value is 1.01 ± 0.04, compared with 1.1 ± 0.1 from previous Voyager data (*24*). Compared with other actively resurfaced icy satellites, Europa's q is marginally higher than that of Enceladus (0.89 ± 0.10) (*25*) but lower than that of Triton (1.14 ± 0.03) (*26*). Using a geometric albedo of 0.67 ± 0.03 for LORRI wavelengths (*8*, *24*), we find a new Bond albedo of 0.68 ± 0.05, compared with a previous value of 0.6 ± 0.1 (*24*), meaning that Europa absorbs less sunlight than previously thought.

References and Notes

1. T. V. Johnson, C. M. Yeats, R. Young, *Space Sci. Rev.* **60**, 3 (1992).
2. F. Bagenal, T. E. Dowling, W. B. McKinnon, Eds., *Jupiter: The Planet, Satellites, and Magnetosphere* (Cambridge Univ. Press, New York, 2004).
3. T. B. McCord *et al.*, *Science* **280**, 1242 (1998).
4. T. B. McCord *et al.*, *J. Geophys. Res.* **104**, 11827 (1999).
5. T. B. McCord, G. B. Hansen, C. A. Hibbitts, *Science* **292**, 1523 (2001).
6. S. A. Stern, *Space Sci. Rev.*, in press; preprint available at http://arxiv.org/abs/0709.4417.
7. D. C. Reuter *et al.*, *Space Sci. Rev.*, in press; preprint available at http://arxiv.org/abs/0709.4281.
8. A. F. Cheng *et al.*, *Space Sci. Rev.*, in press; preprint available at http://arxiv.org/abs/0709.4278.
9. F. P. Fanale *et al.*, *J. Geophys. Res.* **106**, 14595 (2001).
10. K. P. Hand, C. F. Chyba, *Icarus* **189**, 424 (2007).
11. R. W. Carlson, R. E. Johnson, M. S. Anderson, *Science* **286**, 97 (1999).
12. R. W. Carlson, M. S. Anderson, R. E. Johnson, M. B. Schulman, A. H. Yavrouian, *Icarus* **157**, 456 (2002).
13. R. W. Carlson, M. S. Anderson, R. Mehlman, R. E. Johnson, *Icarus* **177**, 461 (2005).
14. J. B. Dalton *et al.*, *Icarus* **177**, 472 (2005).
15. R. E. Johnson *et al.*, in *Jupiter: The Planet, Satellites, and Magnetosphere*, F. Bagenal, T. E. Dowling, W. B. McKinnon, Eds. (Cambridge Univ. Press, New York, 2004), pp. 485–512.
16. A. S. McEwen, *J. Geophys. Res.* **91**, 8077 (1986).
17. W. M. Grundy, B. Schmitt, *J. Geophys. Res.* **103**, 25809 (1998).
18. P. M. Schenk, C. R. Chapman, K. Zahnle, J. M. Moore, in *Jupiter: The Planet, Satellites, and Magnetosphere*, F. Bagenal, T. E. Dowling, W. B. McKinnon, Eds. (Cambridge Univ. Press, New York, 2004), pp. 427–456.
19. P. M. Schenk, *Lunar Planet. Sci. Conf.* **36**, 2081 (2005).
20. R. Greeley *et al.*, in *Jupiter: The Planet, Satellites, and Magnetosphere*, F. Bagenal, T. E. Dowling, W. B. McKinnon, Eds. (Cambridge Univ. Press, New York, 2004), pp. 329–362.
21. A. C. Leith, W. B. McKinnon, *Icarus* **120**, 387 (1996).
22. A. R. Sarid *et al.*, *Icarus* **158**, 24 (2002).
23. P. M. Schenk, I. Matsuyama, F. Nimmo, Lunar and Planetary Institute's "Ices, Oceans, and Fire: Satellites of the Outer Solar System" meeting, Boulder CO, 3 to 15 August 2007, abstract 6090 (2007); available at www.lpi.usra.edu/meetings/icysat2007/pdf/6090.pdf.
24. B. J. Buratti, J. Veverka, *Icarus* **55**, 93 (1983).
25. B. J. Buratti, J. Veverka, *Icarus* **58**, 254 (1984).
26. J. Hillier *et al.*, *Science* **250**, 419 (1990).
27. G. B. Hansen, T. B. McCord, *J. Geophys. Res.* **109**, E01012 (2004).

28. We thank the entire New Horizons mission team and our colleagues on the New Horizons science team. New Horizons is funded by NASA, whose financial support we gratefully acknowledge. We also thank C. A. Hibbits, J. B. Dalton III, G. B. Hansen, and K. Stephan for valuable scientific discussions as well as providing examples of NIMS data.

Supporting Online Material

www.sciencemag.org/cgi/content/full/318/5848/234/DC1
Table S1

10 July 2007; accepted 21 September 2007
10.1126/science.1147623

REPORT

Io's Atmospheric Response to Eclipse: UV Aurorae Observations

K. D. Retherford,[1]* J. R. Spencer,[2] S. A. Stern,[3] J. Saur,[4] D. F. Strobel,[5] A. J. Steffl,[2] G. R. Gladstone,[1] H. A. Weaver,[6] A. F. Cheng,[3] J. Wm. Parker,[2] D. C. Slater,[1] M. H. Versteeg,[1] M. W. Davis,[1] F. Bagenal,[7] H. B. Throop,[2] R. M. C. Lopes,[8] D. C. Reuter,[9] A. Lunsford,[9] S. J. Conard,[6] L. A. Young,[2] J. M. Moore[10]

The New Horizons (NH) spacecraft observed Io's aurora in eclipse on four occasions during spring 2007. NH Alice ultraviolet spectroscopy and concurrent Hubble Space Telescope ultraviolet imaging in eclipse investigate the relative contribution of volcanoes to Io's atmosphere and its interaction with Jupiter's magnetosphere. Auroral brightness and morphology variations after eclipse ingress and egress reveal changes in the relative contribution of sublimation and volcanic sources to the atmosphere. Brightnesses viewed at different geometries are best explained by a dramatic difference between the dayside and nightside atmospheric density. Far-ultraviolet aurora morphology reveals the influence of plumes on Io's electrodynamic interaction with Jupiter's magnetosphere. Comparisons to detailed simulations of Io's aurora indicate that volcanoes supply 1 to 3% of the dayside atmosphere.

Io is a volcanically active moon of Jupiter, and its volcanism is the ultimate source of material for Io's sulfur-dioxide atmosphere. The interaction between Io's atmosphere and the Io plasma torus produces displays of auroral emissions on Io, supplies plasma to Jupiter's magnetosphere, and physically links Io to Jupiter (*1*). The relative importance of the volcanoes as a direct, immediate source of the atmosphere, versus sublimation of frosts deposited around these volcanoes, has remained uncertain since the atmosphere's discovery in 1979 (*2*, *3*). Io's average dayside surface temperature rapidly drops after eclipse ingress or at night [likely from ~120 K to ~90 K; (*4*, *5*)], which is sufficient to diminish the sublimation component of the atmosphere across most of the surface and possibly results in an atmosphere mostly supplied directly from volcanoes.

Aurora observations, particularly while Io is in solar eclipse by Jupiter, can provide information on both Io's atmosphere and its interaction with Jupiter (*6*–*14*). The New Horizons (NH) spacecraft was able to observe Io in eclipse four times during its flyby of Jupiter in late February and early March 2007 (Table 1).

We report NH Alice ultraviolet (UV) spectrometer (*15*) observations of Io eclipse ingress and egress. Io eclipse observations by other NH instruments are reported separately (*16*, *17*). Alice provides spectral images in the extreme- and far-UV (EUV and FUV) pass-bands from 52 nm to 187 nm with 0.3- to 0.4-nm resolution for point sources and 1.0- to 1.2-nm resolution for extended sources, as Io was for our observations (*18*), and a spatial resolution of 0.1° by 0.3° along the 4° long narrow part of its slit.

Supporting observations were also made with the Advanced Camera for Surveys Solar Blind Channel (ACS/SBC) (*19*) on the Hubble Space Telescope (HST). Angular plate scales of 0.034 arc sec/pixel and 0.030 arc sec/pixel on the detector result in slightly rectangular pixels. Use of the SBC's F125LP filter excludes sky background signal from geocoronal Lyman-α emissions while passing through the atomic oxygen (OI) 130.4 nm and longer FUV emissions of interest for Io.

Auroral emission features include a global limb glow around the disk of the satellite, sub-Jupiter and anti-Jupiter equatorial spots (or glows), and a wake region (on the orbital leading hemisphere, down-